

Approaches used for pixel based time series analysis of Landsat data

Literature Review

Version 1.1

Mariela Soto-Berelov, Samuel Hislop

3/18/2016

This literature review is an internal document that will be maintained during the life of the project. The primary purpose is to outline the key processing steps required for pixel-based time series analysis. This document will assist the project research team with the development of time series based algorithms within the context of the project.

Project 4.104, LandFor, A Monitoring and Forecasting Framework for the Sustainable Management of SE Australian Forests at the Large Area Scale

1. Introduction

Forests offer a range of ecosystem services that contribute to the environmental, social, and economic wellbeing of an area (Department of Environment and Primary Industries 2014). To sustainably maintain forests and track their status, land management agencies throughout the world have become signatory to international charters such as the Montreal Process Working Group. Signatory parties are required to report across a range of economic, environmental and social indicators and criteria periodically. Remote sensing has been identified as a suitable tool that can assist forest inventorying and reporting.

One of the most basic yet fundamental attributes is forest cover or forest extent, as it is essential when reporting across any other forest related variable. Equally as important is forest cover change or disturbance, which occurs as part of natural cyclical processes (e.g., phenology) or can be the result of stochastic events. These last can occur abruptly in space and time (e.g., wildfire, logging) or gradually (e.g., drought, succession or recovery, disease, insect outbreak).

Forest cover change can be efficiently captured using remote sensing technology. The last 15 years or so have seen the launch of hyper-temporal remote sensors with spectral bands that target vegetation. These can be used to efficiently monitor changes occurring from regional to global levels but lack sufficient detail for detecting changes occurring at a land management scale. Changes that occur at a more local scale can be successfully and efficiently detected using medium resolution satellite imagery such as Landsat (Townshend and Justice 1988; Wulder et al. 2008), although gradual changes can be harder to detect (Kennedy et al. 2012, Senf et al. 2015) given they are lower in magnitude and can be confused with background noise. In addition, Landsat imagery is available for over 40 years; thus allowing for detailed retrospective forest characterisation. This can help understand trends and bring light to present day forest dynamics (Wulder et al. 2012).

Change detection methods have evolved from mapping and identifying change between image pairs to novel techniques based on dense time series image datasets. Generally speaking, these time series techniques can be grouped into two types, the first group seeking to capture deviations from a stable condition while the second group, which has been receiving increasing attention in recent years, captures change signals associated with processes occurring on the ground after filtering out intra-year or year to year noise introduced by factors including sun angle, sensor drift, haze and phenology.

The large volumes of data being generated by hyper-temporal remote sensors as well as new open data policies that provide access to several decade long image repositories (e.g., USGS opened the Landsat time series archive to the public in 2008) and improved computing, processing and storage capabilities have prompted the development of new change detection algorithms based on dense time series. In addition to detecting and quantifying change, the increased time series allows trends and rates of change to also be identified using pixel or object based methods (Gómez et al. 2015; Kennedy, Yang, and Cohen 2010; Udelhoven 2011; Verbesselt, Zeileis, and Herold 2012a). This literature review focuses on pixel based time series change detection methods that seek to characterize forest disturbance at the land management scale.

2. Pixel based time series analysis

Multiple pixel based time series approaches have been designed and tested in the last decade to detect land use and land cover change at high temporal scales (Table 1). Although different, they all essentially follow a number of general steps outlined in Figure 1. After the initial pre-processing and preparation of the imagery into a stack (Landsat time series stack or LTSS), a metric (or several) is chosen to extract the spectral trajectory of a pixel over time and detect trends. Thirdly, the time series is calibrated (i.e., the trend is fit), and subsequently change is inferred by attributing a change parameter such as year of disturbance, per cent disturbance or magnitude of disturbance. Finally, the model is validated to obtain a measure of the model's accuracy. In some cases, this last step is an iterative stage within the workflow that informs disturbance attribution (validation data can also be used to train the model).

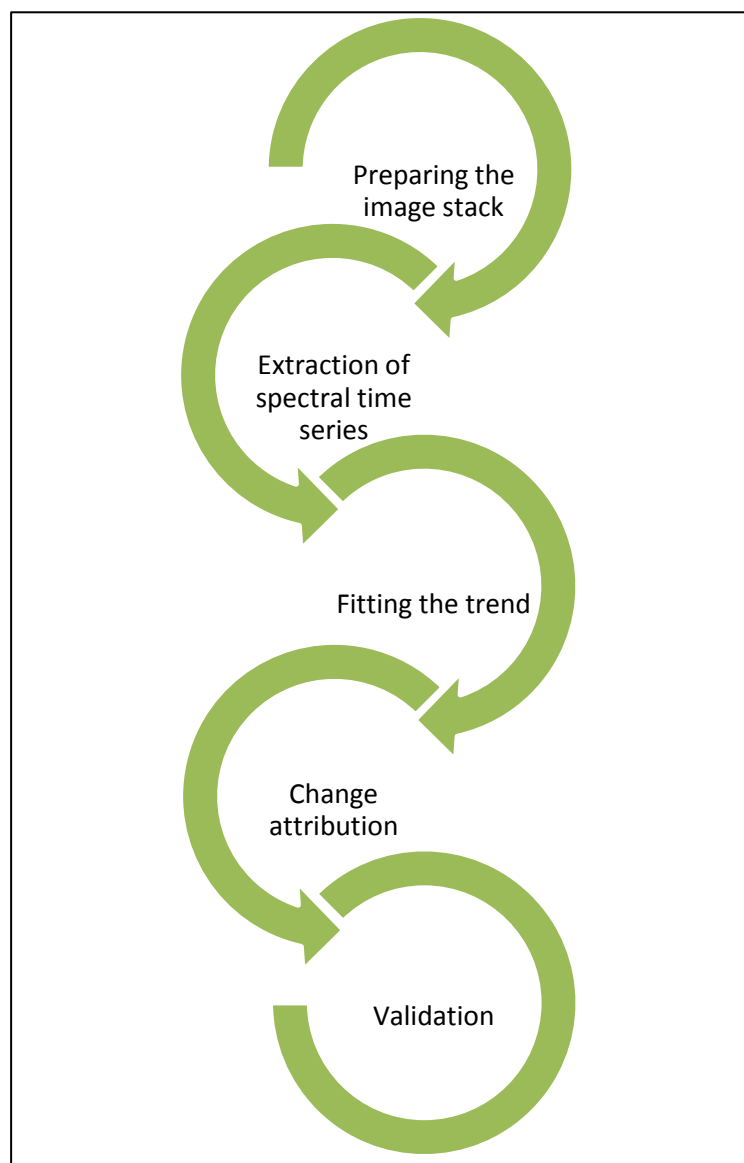


Figure 1. Conceptual diagram outlining the key steps followed during pixel based time series analysis.

Table 1. Examples from the literature of pixel based change detection methods targeting forest areas that are based on dense Landsat time series.

Time series method	Context	Preparing the image stack			Extracting the spectral trajectory		Fitting the trend	Change parameter detected	Validation	Study
		Input data	Temporal resolution	Spatial extent	Index used	Filtering/ Miss registration				
Land TrendR	Evaluate an algorithm for detecting disturbance and recovery trends using time series data	COST (surface reflectance)	Annual composites 1985 to 2007	4 areas within 4 Landsat tiles in the Pacific northwest USA	Single or multiple (in which case one is used as base) Tasseled cap NDVI NBR	Used a tie point selection algorithm to locate 200-500 tie points per image for orthorectification (Kennedy and Cohen 2003)	Automated trajectory based image analysis that allows user input to segment time series into change events occurring through time Segmentation of time series into temporal trajectory	Year of event (disturbance timing) Magnitude of event (% disturbance) Duration of event Recovery magnitude post event Onset year	Reference dataset using TimeSync. Vertices compared (how well algorithms match timing and direction of turning points in trajectory). Also evaluate match in shape of overall trajectory.	(Kennedy et al. 2010)
	Identify defoliator and bark beetle disturbance and recovery	LEDAPS	Annual composites 1990-2013	8 Landsat tiles individually processed and then mosaicked	NBR TC	NMA	Spectral trajectories fitted to NBR and TC time series Two random forests trained to distinguish insect disturbance from fire and logging and attribute disturbance to most likely agent	Disturbance magnitude Disturbance duration Recovery magnitude and duration	Random forest validated with out-of-bag confusion matrix from where overall, user's, producer's accuracy and errors of commission/ omission were derived.	(Senf et al. 2015)
	Compare spectral trajectories of forest recovery across an ecozone	LEDAPS FMASK	Annual composites 1984-2013	8 Landsat tiles 1220 scenes Boreal Shield Ecozone	TC Wetness	NA	Spectral trajectories fitted to TC-Wetness time series to identify disturbance.	Rate of recovery after severe disturbance (fire and logging)	NA	(Frazier, Coops, and Wulder 2015)
	Identify disturbance associated with insect disturbance	L1T COST (surface reflectance) MADCAL (normalize images)	1984-2007	2 Landsat tiles Pacific Northwest	NBR	NA	Spectral trajectories fitted to NBR time series	Absolute magnitude of disturbance Onset year Duration	Used field plots to link trajectories to agents	(Meigs, Kennedy, and Cohen 2011)
BFAST	Forest disturbance at small land holder scale	L1T cloud < 70% LEDAPS FMASK	1992-2012 All available	1 Landsat tile Tropical montane forest SW Ethiopia	NDVI	NA	Iteratively fits a piecewise linear trend and seasonal model that detects break points during 3 stages: 1) fitting (e.g., OLS) a harmonic model based on observations within a defined period; 2) testing observations in monitoring period immediately after the history period for structural breaks from the fitted harmonic model (e.g., using moving sums for all observations); 3) calculating the median of residuals for expected and actual observations within the monitoring period.	Disturbance year and magnitude	Validated 2009 changes. Reference dataset built from a stratified random sample from two populations of pixels: those with and with no change in 2009.	(DeVries, Decuyper, et al. 2015a)
	Near real-time disturbance detection regional	MODIS NDVI 16 day composites MOD13C1	2000-2011	Simulated data and draught affected regions of Somalia	NDVI	Multiple disturbance observations are needed to account for noise		deviation from stable history period	The model was trialled using simulated data, and then tested with a real world example, to detect drought in Somalia	(Verbesselt, Zeileis, and Herold 2012b)

Time series method	Context	Preparing the image stack			Extracting the spectral trajectory		Fitting the trend	Change parameter detected	Validation	Study
		Input data	Temporal resolution	Spatial extent	Index used	Filtering/ Miss registration				
Modified version of BFAST	Monitor forest cover loss	LEDAPS	All available	Dry tropical forest in lowland Bolivia	Two time series indices used as regressors: NDVI Standard Precipitation Index (SPI)	NA	Used two external regressors (variables) to facilitate the discrimination of natural versus human changes: NDVI derived from MODIS with varying window size and SPI from TRMM satellite	Disturbance date	Ground truth samples manually interpreted using TimeSync environment (using visually interpreted Landsat time-series and recent Very High Resolution imagery)	(Dutrieux et al. 2015a)
BFAST & MultiFuse (time series correlation & fusion)	Detect deforestation in plantation in tropics in Fiji	SAR Landsat L1T LEDAPS	All available 2008-2009	1 Landsat tile	NDVI	NA	Optimised regression model used to predict and fuse two time series (derived from SAR and Landsat)	Disturbance date Disturbance magnitude	3-monthly referenced data for whole spatial/temporal scale used for validation	(Reiche et al. 2015a)
Modified version of BFAST that includes MOSUM,	Track disturbance-regrowth in tropical forest	LEDAPS	All available imagery 1990-2014 (1-year monitoring periods)	2 Landsat tiles	NDMI	5-pixel sieve	After using BFAST to monitor forest disturbance at annual timescale, identified regrowth by observing the moving sums (MOSUM) of the residuals against a statistically defined stability boundary	Disturbance date Onset of regrowth Re-clearing date	Human-interpreter approach	(DeVries, Decuyper, et al. 2015b)
Vegetation change tracker (VCT)	Forest disturbance and recovery	Raw images	Biennial 1984-2006	7 forests across eastern US 7 Landsat tiles	Spatially defined forest probability index	Images were geometrically corrected to within one TM pixel prior to time series analysis	Change detection based on hierarchical approach and decision rules derived in a 2-step process: 1. Individual image masking and identification of forest samples used to normalize image radiometry. Forest indices derived across samples. 2. Time series is done using indices and masks for all images in time series using forest likelihood (integrated forest Z scores derived from time series).	Disturbance year Disturbance magnitude	Visual inspection of Landsat images	(Huang et al. 2009)
	Forest disturbance history	L1G LEDAPS	Biennial 1984-2006	USA	NBRI	Images registered to a baseline image and orthorectified			Qualitative (field visits) and quantitative (visual check of a stratified random sample of pixels) accuracy assessment over 6 validation sites	Huang et al. 2010
Modified version of VCT	Characterise forest recovery trends associated with a range of spectral indicators	LEDAPS < 40% cloud cover	Annual composite 1985-2010	40 Landsat tiles across 3 major bioclimatic zones in NA boreal forests	Disturbance index	NA	Applies trend logic to a spectral index using a threshold.	Year of disturbance Disturbance magnitude	Training areas identified using MOD44B for 2000, annual NDVI and visual interpretation of RGB Landsat composites	(Pickell et al. 2016)
VegMachine	Generate time-series summary of vegetation change	Landsat raw	1989-2006 Annual	Continental Australia	Vegetation density index	Images were orthorectified and matched	Summary statistics (e.g., quadratic curvature, slope) are extracted from the vegetation index over time using regression. Linear and quadratic components are estimated by fitting polynomials.	Timing, direction (decline or increase), magnitude, spatial extent of change	Images and products processed by operators were independently checked	(Lehmann et al. 2013)

Time series method	Context	Preparing the image stack			Extracting the spectral trajectory		Fitting the trend	Change parameter detected	Validation	Study
		Input data	Temporal resolution	Spatial extent	Index used	Filtering/ Miss registration				
STARFM Gao et al. 2006	Quantifying land cover change in open forests	97 Landsat (TM: 69 and ETM+: 28) and 525 MODIS	All available data 2000 to 2011	ILCP Research Area, central southeast Queensland. Southern savanna region - forests and agricultural. (37x60km)	NDVI, BRDF, BRDF/Albedo	NA	STARFM combines Landsat (high spatial) with MODIS (high temporal) to produce an interpolated time series with 8 day interval. BFAST was applied to detect breaks	disturbance (clearing events). BFAST applied to NDVI time series extracted from STARFM data	true colour aerial imagery and LIDAR. SLATS annual forest clearing data layers	(Schmidt et al. 2015a)
STAARCH	Produce synthetic imagery and detect changes at fine temporal resolution through data fusion	Landsat MODIS	Landsat (beginning and end of period) MODIS All available 2002-2005	1 Landsat tile west-central Alberta, Canada	Tasseled cap	NA	Change mask derived from Landsat scenes. Temporal evolution of disturbance events extracted from MODIS stack. Surface reflectance extracted from modified version of STARFM.	Disturbance date	Results compared to validation disturbance dataset with dates and location of disturbance events throughout study period. Also compared estimated surface reflectance with Landsat observations from 2004.	(Hilker et al. 2009)
Multi-temporal RGB color composite analysis	Identify fire and harvesting in disturbance events	LEDAPS	Near annual (growing season May-Sept), one image per year	1 Landsat tile	Tested bands linked to forest structure (B5, Tasseled Cap Wetness, forestness index) and leaf greenness (NDVI, NBR, TCA)	NA	Analyst driven, multi-temporal RGB color composite change detection approach	Year and type of forest disturbance	Independent design based accuracy assessment based on visual interpretation	(Schroeder et al. 2011)
Hybrid method	Determine if significant changes have occurred and if so identify if they are gradual or abrupt	>90% cloud free	Eight autumnal scenes 1988-2006	1 Landsat tile Confier forest in wilderness area in northern New Mexico, USA	SWIR/NIR NDVI	NA	Rule set based on pixel values over time.	Time of disturbance Rate of disturbance	Image trends compared with aerial sketch mapping data and field visit	(Vogelmann, Tolk, and Zhu 2009)
Hybrid method (comparison and use of disturbance index)	Map forest disturbance, recovery, & changes in forest type	L1T LEDAPS	Five yearly 1985-2000	Regional composites Carpathians in Eastern Europe	Disturbance Index	NA	Method consists of radiometric change classification and post-classification comparison & continuous index and segment-based post disturbance recovery assessment	Disturbance year Disturbance recovery Disturbance rate	Point based accuracy assessment using forest inventory data and ground truth data	(Patrick Griffiths et al., 2014)
Forest probability	Forest change monitoring Tropics	L1T and L1G	All available 2000-2005	National 81 Landsat tiles	Forest probability determined on per pixel basis in feature space using the SWIR band	NA	Per-pixel decision tree algorithm trained with a binary dataset (forest cover loss and no loss) derived from photo interpreted images. Models fit using an independent reference dataset.	Per-pixel probability of forest cover loss	Independent reference dataset having sample based estimates of forest cover loss	(Broich et al. 2011)

Time series method	Context	Preparing the image stack			Extracting the spectral trajectory		Fitting the trend	Change parameter detected	Validation	Study
		Input data	Temporal resolution	Spatial extent	Index used	Filtering/ Miss registration				
CCDC	Detect land cover change	L1T	All available (519 scenes) 1982-2011 < 80% cloud cover	1 Landsat tile New England	All Landsat spectral bands are used	NA	Model coefficients fit with OLS on remaining clear Landsat observations.	Temporal trajectory based method for all available time series based on modeled historical time series.	Random stratified sample, with 250 pixels in areas of persistent land cover and 250 within areas of change	(Zhu and Woodcock 2014)
CMFDA	Forest disturbance	Landsat ETM+ 2001 to 2002 LEDAPS	All available	60km x 60km Savannah River basin on the border of Georgia and South Carolina	NDVI, band 3 reflectance, band 7 reflectance, NBR, Wetness and B-(G+W)	Noise and mis-registration reduced using multiple temporal observations, ie, for pixel to change it needs to be observed in multiple successive images	Surface reflectance models for each pixel based on OLS fitting. Essentially CMFDA predicts the state of a pixel at any given time and then that prediction is compared to the actual. Multi-date differencing chosen as final change detection method.	Detect forest disturbance with single-date and multi-date differencing. Change index B-(G+W) with threshold of 0.12	Manual assessment of Landsat and other imagery (e.g., Google Earth)	(Zhu, Woodcock, and Olofsson 2012a)

2.1 Pre-processing (characteristics of input image stack)

Landsat pixel based time series change detection methods are applied to specific tiles defined by path/row of the World Reference System (WRS) or to large areas that contain multiple tiles (Broich et al. 2011; White et al. 2014). The images, obtained for the analysis period, are stacked into specific time intervals using specified rules. The temporal interval can be seasonal (Roy et al. 2010), annual (Gómez et al. 2015; Huang et al. 2009; Schmidt et al. 2015b; Zhu and Woodcock 2014), or multi-year (Huang et al. 2009; Potapov, Turubanova, and Hansen 2011). Annual and seasonal images consist of a representative image or an image composite made from the best available pixels within a pre-defined seasonal window (Kennedy et al. 2010; Senf et al. 2015; White et al. 2014).

Restricting imagery to a particular season can minimize reflectance discrepancies caused by phenology, haze, and sun angle differences (Flood 2013) and capture change at seasonal and yearly time scales (Flood 2013). Although intra-year changes are undetected, this may actually be an advantage as such changes could be considered to be noise when looking at multiple year time series datasets (Kennedy et al. 2010). In addition, seasonal and annual composites reduce the volume of data, which is an important consideration when doing long term time series across large areas that consist of multiple Landsat tiles. In this way, only one (annual) or four (seasonal) images (with one value per band) are needed per tile, as opposed to hundreds if analysing change using all available imagery (Landsat has a 16-day revisit cycle). Nevertheless and depending on the context, it may be preferable to take advantage of all available imagery within a given time period and in this way detect changes occurring at finer temporal resolutions (Broich et al. 2011; DeVries, Decuyper, et al. 2015b; Zhu et al. 2012a). These include changes associated with forest harvest cycles, phenological dynamics, and post-disturbance regrowth dynamics (DeVries, Decuyper, et al. 2015b; Schmidt et al. 2015b).

To minimise noise introduced from data gaps, shadows, clouds, etc., while exploiting all available imagery, compositing approaches are applied¹. A series of compositing approaches have emerged over the last decade and a summary of these is provided in (White et al. 2014). Image composites can be created using the best-available-pixel (BAP) paradigm (Kennedy et al. 2010; White et al. 2014), which is based on user-defined rules applied to the Landsat archive to generate large area image composites that are cloud-free, radiometrically and phenologically consistent (Griffiths et al. 2013; Roy et al. 2010; White et al. 2014). For instance, White et al. (2014) provide criteria for ranking pixels acquired by multiple scenes on the basis of sensor (e.g., Landsat TM can have a higher score than Landsat ETM+ due to SLC-gaps), day-of-year, atmospheric opacity and presence/closeness to cloud or shadow. Pixels that obtain the highest scores can be used to create composites (Pickell et al., 2016). To sidestep data gaps, Huang et al. (2010) altogether avoided images from Landsat ETM+ post May 2003 (SLC-off) and created biennial composites using temporal interpolation. This last considers pixels that are closest in time to when the gaps occurred (Hermosilla et al. 2015a; Huang et al. 2010; Schroeder et al. 2011). Additional criteria used by others to select BAP include choosing the greenest pixel within a pre-defined period; using median value compositing rules (Broich et al. 2011); the maximum value of NDVI (Dennison, Roberts, and Peterson 2007); a multi-dimensional

¹ In some instances, the presence of clouds, shadows, haze and other factors can considerably limit image availability. Also in 2003, the Scan Line Corrector (SLC) of Landsat 7 ETM+ failed and as a result, gaps need to be masked and replaced.

median (Flood 2013) or using both temporal and spatial information to predict missing values (Wang et al. 2012).

Furthermore, operational tools have been developed to derive gap-free surface reflectance images and mask unwanted noise. An example is LEDAPS (P Griffiths et al., 2013; Schmidt, G., Jenkerson, C., Masek, J., Vermote, E., Gao, 2013), which provides a tool chain with embedded cloud masking (Fmask (Zhu, Woodcock, and Olofsson 2012b)) for deriving surface reflectance of Landsat TM and ETM. It consists of a weighted pixel-based scoring system based on acquisition year, day of year, and distance of a given pixel to a cloud. LEDAPS has been applied on Landsat Level-1 Terrain Corrected (L1T) products which have been processed to surface reflectance and can be immediately accessed through the USGS website (these products are known as Climate Data Records or CDR). Rules can then be applied to create composites that exploit gap-free observations obtained during specific intervals.

2.1.1 Pixel misregistration

Images that have not been geometrically corrected can cause pixel misregistration and introduce errors when extracting a pixel's trajectory (Huang et al. 2009). Images acquired after the Landsat archive became publically available tend not to have sub-pixel registration errors and usually do not require further geometric processing (Kennedy et al. 2010) given advanced correction methods have been implemented as automated modules in LEDAPS. Nevertheless, images can be co-registered to a baseline image and/or orthorectified to avoid errors caused by terrain relief (Huang et al. 2010).

As a compromise between spatial detail and pixel misregistration, a window kernel centred on the pixel of interest can also be used (Kennedy et al. 2010). DeVries et al. (DeVries, Decuyper, et al. 2015b) found that filtered cloud pixels adjacent to masked SLC-gap pixels were frequently missed, so they applied a 5-pixel sieve on each scene. Kennedy et al. (Kennedy et al. 2010) chose the mean value in a 3 by 3 window.

2.2 Extracting the spectral trajectory

Once representative images have been stacked, the temporal spectral trajectory of a pixel is extracted using a particular metric or index (or several) derived from a subset of bands present in the Landsat sensor. Table 2 lists the bands used in Landsat Thematic Mapper (TM) and Enhanced Thematic Mapper Plus (ETM+) sensors, the two most commonly used Landsat sensors in pixel-based time series analysis.

Table 2. Spectral bands of Landsat Thematic Mapper (TM) and Enhanced Thematic Mapper Plus (ETM+) commonly used throughout the literature to detect and map forest disturbance. The approximate scene size of a Landsat scene is 170 km north-south by 183 km east-west and the spatial resolution (IFOV) is 28.5 m.

Band number	Region in the electromagnetic spectrum	Wavelength (micrometers)
Band 1 (B1)	Visible blue	0.45-0.52
Band 2 (B2)	Visible green	0.52-0.60
Band 3 (B3)	Visible red	0.63-0.69
Band 4 (B4)	Near infrared	0.76-0.90 (TM) 0.77-0.90 (ETM+)
Band 5 (B5)	Mid infrared	1.55-1.75
Band 6 (B6)	Thermal infrared	10.40-12.50
Band 7 (B7)	Mid infrared	2.08-2.35 (TM) 2.09-2.35 (ETM+)

Some commonly used indices and metrics are shown in Table 3. These essentially fall into two categories, based on whether the focus is on forest structure or greenness. The first group exploit the short-wave infrared (SWIR) region and include B5, Tasseled Cap Wetness (also shown to be insensitive to topographically induced illumination angle (Cohen and Spies 1992)), Normalized Difference Moisture Index or NDMI, and the Forestness Index or FI (Huang et al. 2009, 2010). These have been shown to be sensitive to forest structure, vegetation density, shadowing and have been successfully used to identify disturbance caused by logging and fire (Schroeder et al. 2011), compare rates of forest recovery after severe disturbance events (Frazier et al. 2015) and detect gradual changes in conifer forests associated with forest damage as well as disturbance-recovery dynamics in tropical forests (DeVries, Decuyper, et al. 2015b).

Table 3. Metrics and indices commonly used to capture trends associated with forest disturbance using dense time series image stacks and or used to monitor recovery after a disturbance event.

Index / Formula	Acronym	Case studies
Normalised Difference Vegetation Index $NDVI = (B4 - B3) / (B4 + B3)$	NDVI	(DeVries, Decuyper, et al. 2015b; Pickell et al. 2016; Reiche et al. 2015b)
Normalized Burn Ratio Index $NBRI = (B4 - B7) / (B4 + B7)$	NBR or NBRI	(Cohen, Yang, and Kennedy 2010; Hermosilla et al. 2015a, 2015b; Huang et al. 2010; Kennedy et al. 2010; Meigs et al. 2011; Pickell et al. 2016; Senf et al. 2015; Zhu et al. 2012a)
Forestness Index (z-score measure of a pixels likelihood of being forested, using B3, B5, B7)	FI	(Huang et al. 2009, 2010)
Normalized Difference Moisture Index or Normalized Difference Water Index $NDMI = (B4 - B5) / (B4 + B5)$	NDMI or NDWI	(DeVries, Decuyper, et al. 2015a; Gao et al. 2013; Goodwin et al. 2010)
Metrics derived from Tasseled Cap transformation: Tasseled Cap angle Wetness Brightness Greenness Disturbance Index	TC TCA TCA-W TCA-B TCA-G DI	(Cohen et al. 2010; Frazier et al. 2015; Kennedy et al. 2010; Pickell et al. 2016; Senf et al. 2015)
B4+B5	B45	(Goodwin and Collett 2014)

Indices and metrics that fall under the greenness category are centred in the near infrared region of the spectrum (B4). One of the most commonly used is the Normalized Difference Vegetation Index (NDVI) given its proven ability to capture changes in forest condition over time (DeVries, Decuyper, et al. 2015b; Dutrieux et al. 2015b; Reiche et al. 2015b). However it is not without its shortcomings given its potential to saturate in dense forests. Other indices that fall in the greenness category include the Normalized Burn Ratio (NBR) and the Tasseled Cap Angle or TCA. NBR has been used to detect insect disturbance (e.g., Meigs et al. 2011, Townsend et al. 2012). The Tassel Cap components, derived in multi-dimensional space, have been found to be sensitive to green

vegetation (Greenness), moisture content (Wetness), background soil (Brightness) and have been used in studies to detect disturbance caused by insect infestation (Senf et al. 2015).

2.3 Fitting the trend

Contrary to bi-temporal change detection methods, time series algorithms analyse the trajectory of an image stack. Several conceptual models have been designed to statistically identify and fit a time series trend within the spectral trajectory of a pixel over time (Table 1). Besides following different statistical approaches, these vary according to their intended use (Dutrieux et al. 2015a) and whether disturbance dynamics occurring in an intra-annual, annual, or multi-annual scale are to be characterised.

A trajectory-based change detection algorithm that analyses all the images present in the time series stack was developed by Kennedy et al. (Kennedy, Cohen, and Schroeder 2007; Kennedy et al. 2010). Changes are detected using the idealized temporal trajectory of spectral values (Huang et al. 2010). In this approach, the spectral trajectories of pixels are divided into a series of interconnected linear segments and fit to the time series through a two-step process that consists of segmentation and model fitting. First during the segmentation, a spectral index is used to estimate stable trajectories and breakpoints that indicate disturbance. The beginning and end of each segment marks a breakpoint in a trajectory and the length of the segment determines its temporal duration. Afterwards, the value of the spectral index used in the segmentation is estimated at each vertex. The disturbance and recovery of identified trajectories are then described through a series of metrics. To attribute disturbance events into meaningful agents of change, reference pixels (randomly selected) are attributed using ancillary datasets (Senf et al. 2015). A model such as Random Forests can then be trained with the reference pixels to attribute all disturbances.

Another method that analyses all images in a time series stack simultaneously is the Vegetation change tracker or VCT (Huang et al. 2009). However, the VCT uses a hierarchical approach and a series of decision rules. First individual images are masked and forest samples are identified (these are used to normalize image radiometry). Forest indices are then derived across the samples. The VCT analyses each image within the stack to mask forests which are assigned a per-pixel forest Z-score index (IFZ) that captures disturbance. This method has also been modified by applying trend logic to a spectral index using a threshold (Pickell et al. 2016).

Other methods focus on detecting changes occurring at finer time scales. An example is the Continuous Monitoring of Forest Disturbances Algorithm or CMFDA (Zhu et al. 2012a), which detects disturbances using Fourier series and a threshold based deviation from the model mechanism. For a change to be detected, three subsequent observations that exceed the threshold are required. Another group of methods that use all available imagery are those that decompose dense time series into seasonal trends. Such methods rest on the idea that a stable time series follows patterns that are historically observed and defined. In other words, the time series requires a “stable” period that will be used as the benchmark against which to measure deviations. Whenever the time series (within defined monitoring periods) deviates from the stable pattern (identified whenever a break point is identified), a disturbance event is inferred. However a threshold is required to distinguish disturbance whenever a positive or negative breakpoint is detected (DeVries, Decuyper, et al. 2015a). An example of such a method is the Breaks for Additive Season and Trend or BFAST Monitor

algorithm (DeVries, Verbesselt, et al. 2015; Verbesselt et al. 2010, 2012a), an iterative algorithm that decomposes pixel time series into several components: season, noise, and trend. It works by deriving a first-order harmonic seasonal model from all data available for a monitoring period and then projecting into the sequential period. This method has been tested with simulated NDVI and real time 16-day MODIS NDVI composites (Verbesselt et al. 2010) and used to detect near real time disturbance (Verbesselt et al. 2012a). It has also been optimised to distinguish anthropogenic versus naturally occurring changes in environments that experience high inter-annual variability (Dutrieux et al. 2015a) and used in conjunction with other structural change detection methods to identify and track disturbance-regrowth dynamics (DeVries, Decuyper, et al. 2015b).

Several other methods are based on probability rules (Vogelmann et al. 2009). Some of these use per-pixel decision tree algorithms that can be fitted using a training set (Broich et al. 2011) derived from ancillary data. In such cases, maps that produce a probabilistic output require a threshold to define forest cover loss. Other methods generate time-series summary information of vegetation change by extracting summary statistics (e.g., quadratic curvature, slope) from a vegetation index over time using regression.

2.4 Extraction of summary information within trend

The attributes used for describing disturbance events vary according to the time series method used (Table 1), although all include an attribute associated with the timing of disturbance. In some cases, a timing when recovery commences as well as the time post disturbance when the forest reaches a stable condition is also produced as an output (DeVries, Decuyper, et al. 2015b). Structural methods that are based on identifying breakpoints that indicate deviations from a stable condition characterize change according to their magnitude and direction (Verbesselt et al. 2010). These report on the magnitude of disturbance (DeVries, Verbesselt, et al. 2015; Verbesselt et al. 2012a) as well as disturbance date, onset of regrowth and re-clearing date (DeVries, Decuyper, et al. 2015a). Other methods report on per cent disturbance, per cent forest cover loss (Broich et al. 2011) duration of disturbance event and magnitude of disturbance (Huang et al. 2009). Using LandTrendR, Senf et al. (2015) also reported the greatest disturbance event in the time series they analysed and attributed per cent change (from change in magnitude) and onset of disturbance (defined as the first year of the greatest disturbance segment).

2.5 Validation

Reference data (e.g., field work or high resolution imagery) traditionally used for validating the accuracy of a satellite derived product can be challenging and impractical when validating a time series disturbance product given reference data may not exist or be limited. Nevertheless, different sources of data and approaches can be applied. Some methods incorporate validation into the general workflow where it is done as an iterative step that feeds into the model calibration. In such cases, ancillary datasets can be used as classifiers (e.g., decision trees, maximum likelihood) for both fitting and evaluating the model (Broich et al. 2011). The validation can also be done applying a human interpreter approach (Cohen et al. 2010; DeVries, Decuyper, et al. 2015b) that has input from ancillary sources (e.g., Google Earth, Rapid Eye, corporate datasets, field plots). This can be executed

over a multi-stage sampling framework that examines randomly selected disturbed and undisturbed pixels or specifically targeted locations.

Tools that facilitate the validation of time series using human interpretation in a semi-automated environment are also being developed and used (Kennedy et al. 2010). An example is TimeSync, a time series visualisation and data collection tool that ensures samples are statistically robust given they are free of temporal and spatial restrictions, unlike traditionally used reference data which is mostly patchy and biased (Cohen et al. 2010).

3. Conclusion

Forests provide a suite of services that are essential for maintaining societal and environmental needs and wellbeing. Land management agencies around the world are tasked with providing up to date information regarding the state of forests. Remote sensing technology has been identified as an essential component in the toolkit used for forest inventorying, monitoring, and reporting activities.

The opening up to the public of the Landsat archive that contains over four decade's worth of earth observation images at a scale capable of detecting changes occurring at a land management scale has prompted a new paradigm of land use and land cover change detection. As a result, various algorithms based on dense Landsat time series stacks have been developed in the last decade to detect trends as well as disturbance and recovery dynamics that impact forests. To ease analysis, several flow chains have been developed to derive surface reflectance from satellite images (Schmidt, G. , Jenkerson, C. , Masek, J., Vermote, E., Gao 2013). As part of this process, masking clouds and other unwanted signals has become operationally feasible.

Time series methods are based on dense intra-annual, seasonal, annual, or multi-annual image composites that are stacked and analysed to detect trends and deviations from a stable condition. They use different approaches to fit the spectral trajectory of pixels and identify disturbance. After detecting disturbance, attribution is mainly achieved using reference datasets that have a strong human-interpreter component. This review has summarised the key steps followed in pixel-based time series analysis. Ultimately the selection of one method over another should be on a case specific basis that examines available imagery, time period, type of disturbance to be detected, desired level of attribution and available reference data.

References

- Broich, Mark et al. 2011. "Time-Series Analysis of Multi-Resolution Optical Imagery for Quantifying Forest Cover Loss in Sumatra and Kalimantan, Indonesia." *International Journal of Applied Earth Observation and Geoinformation* 13(2):277–91. Retrieved (<http://linkinghub.elsevier.com/retrieve/pii/S0303243410001340>).
- Cohen, Warren B., and Thomas A. Spies. 1992. "Estimating Structural Attributes of Douglas-Fir/western Hemlock Forest Stands from Landsat and SPOT Imagery." *Remote Sensing of Environment* 41(1):1–17.
- Cohen, Warren B., Zhiqiang Yang, and Robert Kennedy. 2010. "Detecting Trends in Forest Disturbance and Recovery Using Yearly Landsat Time Series: 2. TimeSync - Tools for Calibration and Validation." *Remote Sensing of Environment* 114(12):2911–24. Retrieved (<http://dx.doi.org/10.1016/j.rse.2010.07.010>).

- Dennison, Philip E., Dar A. Roberts, and Seth H. Peterson. 2007. "Spectral Shape-Based Temporal Compositing Algorithms for MODIS Surface Reflectance Data." *Remote Sensing of Environment* 109(4):510–22.
- Department of Environment and Primary Industries. 2014. *Victoria 'S State of the Forests Report 2013*.
- DeVries, Ben, Mathieu Decuyper, et al. 2015a. "Tracking Disturbance-Regrowth Dynamics in Tropical Forests Using Structural Change Detection and Landsat Time Series." *Remote Sensing of Environment* 169:320–34. Retrieved (<http://linkinghub.elsevier.com/retrieve/pii/S0034425715301061>).
- DeVries, Ben, Mathieu Decuyper, et al. 2015b. "Tracking Disturbance-Regrowth Dynamics in Tropical Forests Using Structural Change Detection and Landsat Time Series." *Remote Sensing of Environment* 169:320–34.
- DeVries, Ben, Jan Verbesselt, Lammert Kooistra, and Martin Herold. 2015. "Robust Monitoring of Small-Scale Forest Disturbances in a Tropical Montane Forest Using Landsat Time Series." *Remote Sensing of Environment* 161:107–21.
- Dutrieux, Loïc Paul, Jan Verbesselt, Lammert Kooistra, and Martin Herold. 2015a. "Monitoring Forest Cover Loss Using Multiple Data Streams, a Case Study of a Tropical Dry Forest in Bolivia." *ISPRS Journal of Photogrammetry and Remote Sensing* 107:112–25. Retrieved (<http://www.scopus.com/inward/record.url?eid=2-s2.0-84928184753&partnerID=tZOtx3y1>).
- Dutrieux, Loïc Paul, Jan Verbesselt, Lammert Kooistra, and Martin Herold. 2015b. "Monitoring Forest Cover Loss Using Multiple Data Streams, a Case Study of a Tropical Dry Forest in Bolivia." *ISPRS Journal of Photogrammetry and Remote Sensing* 107:112–25.
- Flood, Neil. 2013. "Seasonal Composite Landsat TM/ETM+ Images Using the Medoid (a Multi-Dimensional Median)." *Remote Sensing* 5(12):6481–6500. Retrieved (<http://www.mdpi.com/2072-4292/5/12/6481/>).
- Frazier, Ryan J., Nicholas C. Coops, and Michael A. Wulder. 2015. "Boreal Shield Forest Disturbance and Recovery Trends Using Landsat Time Series." *Remote Sensing of Environment* 170:317–27. Retrieved (<http://linkinghub.elsevier.com/retrieve/pii/S0034425715301383>).
- Gao, Yanhua et al. 2013. "Estimation of the North–South Transect of Eastern China Forest Biomass Using Remote Sensing and Forest Inventory Data." *International Journal of Remote Sensing* 34(15):5598–5610. Retrieved August 7, 2013 (<http://www.tandfonline.com/doi/abs/10.1080/01431161.2013.794985>).
- Gómez, Cristina, Joanne C. White, Michael A. Wulder, and Pablo Alejandro. 2015. "Integrated Object-Based Spatiotemporal Characterization of Forest Change from an Annual Time Series of Landsat Image Composites." 1–44.
- Goodwin, Nicholas R., and Lisa J. Collett. 2014. "Development of an Automated Method for Mapping Fire History Captured in Landsat TM and ETM+ Time Series Across Queensland, Australia." *Remote Sensing of Environment* 148:206–21. Retrieved (<http://www.sciencedirect.com/science/article/pii/S0034425714001072>).
- Goodwin, Nicholas R., Steen Magnussen, Nicholas C. Coops, and Michael a. Wulder. 2010. "Curve Fitting of Time-Series Landsat Imagery for Characterizing a Mountain Pine Beetle Infestation." *International Journal of Remote Sensing* 31(12):3263–71.

- Griffiths, P., S. van der Linden, T. Kuemmerle, and P. Hostert. 2013. "A Pixel-Based Landsat Compositing Algorithm for Large Area Land Cover Mapping." *Selected Topics in Applied Earth Observations and Remote Sensing, IEEE Journal of PP*(99):1–14. Retrieved (<http://ieeexplore.ieee.org/xpl/articleDetails.jsp?arnumber=6415303>).
- Griffiths, Patrick et al. 2014. "Forest Disturbances, Forest Recovery, and Changes in Forest Types across the Carpathian Ecoregion from 1985 to 2010 Based on Landsat Image Composites." *Remote Sensing of Environment* 151:72–88. Retrieved (<http://www.sciencedirect.com/science/article/pii/S0034425713003453>).
- Hermosilla, Txomin, Michael A. Wulder, Joanne C. White, Nicholas C. Coops, and Geordie W. Hobart. 2015a. "An Integrated Landsat Time Series Protocol for Change Detection and Generation of Annual Gap-Free Surface Reflectance Composites." *Remote Sensing of Environment* 158:220–34. Retrieved (<http://linkinghub.elsevier.com/retrieve/pii/S0034425714004453>).
- Hermosilla, Txomin, Michael A. Wulder, Joanne C. White, Nicholas C. Coops, and Geordie W. Hobart. 2015b. "Regional Detection, Characterization, and Attribution of Annual Forest Change from 1984 to 2012 Using Landsat-Derived Time-Series Metrics." *Remote Sensing of Environment* 170:121–32. Retrieved (<http://linkinghub.elsevier.com/retrieve/pii/S0034425715301279>).
- Hilker, Thomas et al. 2009. "Generation of Dense Time Series Synthetic Landsat Data through Data Blending with MODIS Using a Spatial and Temporal Adaptive Reflectance Fusion Model." *Remote Sensing of Environment* 113(9):1988–99. Retrieved (<http://linkinghub.elsevier.com/retrieve/pii/S0034425709001709>).
- Huang, Chengquan et al. 2009. "Dynamics of National Forests Assessed Using the Landsat Record: Case Studies in Eastern United States." *Remote Sensing of Environment* 113(7):1430–42. Retrieved (<http://linkinghub.elsevier.com/retrieve/pii/S0034425709000571>).
- Huang, Chengquan et al. 2010. "An Automated Approach for Reconstructing Recent Forest Disturbance History Using Dense Landsat Time Series Stacks." *Remote Sensing of Environment* 114(1):183–98. Retrieved (<http://dx.doi.org/10.1016/j.rse.2009.08.017>).
- Kennedy, R. E., and W. B. Cohen. 2003. "Automated Designation of Tie-Points for Image-to-Image Coregistration." *International Journal of Remote Sensing* 24(17):3467–90.
- Kennedy, Robert E., Warren B. Cohen, and Todd A. Schroeder. 2007. "Trajectory-Based Change Detection for Automated Characterization of Forest Disturbance Dynamics." *Remote Sensing of Environment* 110(3):370–86. Retrieved (<http://linkinghub.elsevier.com/retrieve/pii/S0034425707001216>).
- Kennedy, Robert E., Zhiqiang Yang, and Warren B. Cohen. 2010. "Detecting Trends in Forest Disturbance and Recovery Using Yearly Landsat Time Series: 1. LandTrendr — Temporal Segmentation Algorithms." *Remote Sensing of Environment* 114(12):2897–2910. Retrieved (<http://linkinghub.elsevier.com/retrieve/pii/S0034425710002245>).
- Lehmann, Eric a., Jeremy F. Wallace, Peter a. Caccetta, Suzanne L. Furby, and Katherine Zdunic. 2013. "Forest Cover Trends from Time Series Landsat Data for the Australian Continent." *International Journal of Applied Earth Observation and Geoinformation* 21:453–62. Retrieved August 8, 2013 (<http://linkinghub.elsevier.com/retrieve/pii/S030324341200133X>).
- Meigs, Garrett W., Robert E. Kennedy, and Warren B. Cohen. 2011. "A Landsat Time Series Approach to Characterize Bark Beetle and Defoliator Impacts on Tree Mortality and Surface Fuels in Conifer Forests." *Remote Sensing of Environment* 115(12):3707–18. Retrieved

(<http://dx.doi.org/10.1016/j.rse.2011.09.009>).

- Pickell, Paul D., Txomin Hermosilla, Ryan J. Frazier, Nicholas C. Coops, and Michael A. Wulder. 2016. "Forest Recovery Trends Derived from Landsat Time Series for North American Boreal Forests." *International Journal of Remote Sensing* 37(1):138–49. Retrieved (<http://www.tandfonline.com/doi/full/10.1080/2150704X.2015.1126375>).
- Potapov, Peter, Svetlana Turubanova, and Matthew C. Hansen. 2011. "Regional-Scale Boreal Forest Cover and Change Mapping Using Landsat Data Composites for European Russia." *Remote Sensing of Environment* 115(2):548–61. Retrieved (<http://dx.doi.org/10.1016/j.rse.2010.10.001>).
- Reiche, Johannes, Jan Verbesselt, Dirk Hoekman, and Martin Herold. 2015a. "Fusing Landsat and SAR Time Series to Detect Deforestation in the Tropics." *Remote Sensing of Environment* 156:276–93. Retrieved (<http://linkinghub.elsevier.com/retrieve/pii/S0034425714003885>).
- Reiche, Johannes, Jan Verbesselt, Dirk Hoekman, and Martin Herold. 2015b. "Fusing Landsat and SAR Time Series to Detect Deforestation in the Tropics." *Remote Sensing of Environment* 156:276–93.
- Roy, David P. et al. 2010. "Web-Enabled Landsat Data (WELD): Landsat ETM+ Composited Mosaics of the Conterminous United States." *Remote Sensing of Environment* 114(1):35–49. Retrieved (<http://dx.doi.org/10.1016/j.rse.2009.08.011>).
- Schmidt, G. , Jenkerson, C. , Masek, J., Vermote, E., Gao, F. 2013. "Landsat Ecosystem Disturbance Adaptive Processing System (LEDAPS) Algorithm Description." *Reston: USGS, 2013* (December):1–27. Retrieved (<http://pubs.usgs.gov/of/2013/1057/>).
- Schmidt, Michael, Richard Lucas, Peter Bunting, Jan Verbesselt, and John Armston. 2015a. "Multi-Resolution Time Series Imagery for Forest Disturbance and Regrowth Monitoring in Queensland, Australia." *Remote Sensing of Environment* 158:156–68. Retrieved (<http://linkinghub.elsevier.com/retrieve/pii/S003442571400457X>).
- Schmidt, Michael, Richard Lucas, Peter Bunting, Jan Verbesselt, and John Armston. 2015b. "Multi-Resolution Time Series Imagery for Forest Disturbance and Regrowth Monitoring in Queensland, Australia." *Remote Sensing of Environment* 158:156–68.
- Schroeder, Todd a., Michael a. Wulder, Sean P. Healey, and Gretchen G. Moisen. 2011. "Mapping Wildfire and Clearcut Harvest Disturbances in Boreal Forests with Landsat Time Series Data." *Remote Sensing of Environment* 115(6):1421–33. Retrieved (<http://dx.doi.org/10.1016/j.rse.2011.01.022>).
- Senf, Cornelius, Dirk Pflugmacher, Michael A. Wulder, and Patrick Hostert. 2015. "Characterizing Spectral–temporal Patterns of Defoliator and Bark Beetle Disturbances Using Landsat Time Series." *Remote Sensing of Environment* 170:166–77. Retrieved (<http://linkinghub.elsevier.com/retrieve/pii/S0034425715301425>).
- Townshend, J. R. G., and C. O. Justice. 1988. "Selecting the Spatial Resolution of Satellite Sensors Required for Global Monitoring of Land Transformations." *International Journal of Remote Sensing* 9(2):187–236. Retrieved (<http://www.tandfonline.com/doi/abs/10.1080/01431168808954847>).
- Udelhoven, Thomas. 2011. "TimeStats: A Software Tool for the Retrieval of Temporal Patterns from Global Satellite Archives." *IEEE Journal of Selected Topics in Applied Earth Observations and Remote Sensing* 4(2):310–17.

- Verbesselt, Jan, Rob Hyndman, Glenn Newnham, and Darius Culvenor. 2010. "Detecting Trend and Seasonal Changes in Satellite Image Time Series." *Remote Sensing of Environment* 114(1):106–15. Retrieved (<http://www.sciencedirect.com/science/article/pii/S003442570900265X>).
- Verbesselt, Jan, Achim Zeileis, and Martin Herold. 2012a. "Near Real-Time Disturbance Detection Using Satellite Image Time Series." *Remote Sensing of Environment* 123:98–108.
- Verbesselt, Jan, Achim Zeileis, and Martin Herold. 2012b. "Near Real-Time Disturbance Detection Using Satellite Image Time Series." *Remote Sensing of Environment* 123:98–108. Retrieved (<http://dx.doi.org/10.1016/j.rse.2012.02.022>).
- Vogelmann, James E., Brian Tolk, and Zhiliang Zhu. 2009. "Monitoring Forest Changes in the Southwestern United States Using Multitemporal Landsat Data." *Remote Sensing of Environment* 113(8):1739–48. Retrieved (<http://dx.doi.org/10.1016/j.rse.2009.04.014>).
- Wang, Guojie, Damien Garcia, Yi Liu, Richard de Jeu, and A. Johannes Dolman. 2012. "A Three-Dimensional Gap Filling Method for Large Geophysical Datasets: Application to Global Satellite Soil Moisture Observations." *Environmental Modelling & Software* 30:139–42. Retrieved (<http://linkinghub.elsevier.com/retrieve/pii/S1364815211002453>).
- White, J. C. et al. 2014. "Pixel-Based Image Compositing for Large-Area Dense Time Series Applications and Science." *Canadian Journal of Remote Sensing* 40(3):192–212. Retrieved (<http://www.tandfonline.com/doi/abs/10.1080/07038992.2014.945827>).
- Wulder, Michael a. et al. 2008. "Landsat Continuity: Issues and Opportunities for Land Cover Monitoring." *Remote Sensing of Environment* 112(3):955–69. Retrieved August 12, 2013 (<http://linkinghub.elsevier.com/retrieve/pii/S0034425707003331>).
- Wulder, Michael a., Jeffrey G. Masek, Warren B. Cohen, Thomas R. Loveland, and Curtis E. Woodcock. 2012. "Opening the Archive: How Free Data Has Enabled the Science and Monitoring Promise of Landsat." *Remote Sensing of Environment* 122:2–10. Retrieved November 5, 2012 (<http://linkinghub.elsevier.com/retrieve/pii/S003442571200034X>).
- Zhu, Zhe, and Curtis E. Woodcock. 2014. "Continuous Change Detection and Classification of Land Cover Using All Available Landsat Data." *Remote Sensing of Environment* 144:152–71. Retrieved (<http://linkinghub.elsevier.com/retrieve/pii/S0034425714000248>).
- Zhu, Zhe, Curtis E. Woodcock, and Pontus Olofsson. 2012a. "Continuous Monitoring of Forest Disturbance Using All Available Landsat Imagery." *Remote Sensing of Environment* 122:75–91. Retrieved May 27, 2013 (<http://linkinghub.elsevier.com/retrieve/pii/S0034425712000387>).
- Zhu, Zhe, Curtis E. Woodcock, and Pontus Olofsson. 2012b. "Continuous Monitoring of Forest Disturbance Using All Available Landsat Imagery." *Remote Sensing of Environment* 122:75–91. Retrieved (<http://dx.doi.org/10.1016/j.rse.2011.10.030>).